Electronic Supplementary Information

A novel cationic-ordering fluoro-polyanionic cathode $LiV_{0.5}Fe_{0.5}PO_4F$ and its single phase Li^+ insertion/extraction behaviour

Zhen-Dong Huang[a],* Yuki Orikasa[a], Titus Masese[a], Kentaro Yamamoto[a], Takuya Mori[a], Taketoshi Minato[b], Yoshiharu Uchimoto[a]

[a]Graduate School of Human and Environmental Studies, Kyoto University, Yoshida-nihonmatsu-cho, Sakyo-ku, Kyoto 606-8501, Japan
[b]Office of Society-Academia Collaboration for Innovation, Kyoto University, Gokasho, Uji 611-0011, Japan

Experimental

Preparation of $LiV_{0.5}Fe_{0.5}PO_4F$ (LVFPF)

Stoichiometric amounts of LiH_2PO_4 (97%, STREM Chemicals), FeF_3 (anhydrous, 99+%, STREM Chemicals) and V_2O_5 (98+%, Sigma-Aldrich) powders corresponding to 0.005 mol of $LiV_{0.5}Fe_{0.5}PO_4F$ were weighed in a molar ratio of 4:2:1. Citric acid (anhydrous, Wako) was introduced as a reductive agent and carbon source. The stoichiometric amounts of the respective precursors were calculated based on the following reactions:

$$2FeF_3+4LiH_2PO_4+V_2O_5+2C \rightarrow 4LiV_{0.5}Fe_{0.5}PO_4F + 3H_2O + 2CO+2HF \quad (1)$$

$$C_6H_8O_7 \rightarrow 3C+ 4H_2O + 3CO \quad (2)$$

To ensure the complete reduction of V^{5+} to V^{3+}, an additional amount of citric acid corresponding to 15% excess carbon was added. The weighed chemicals were sealed into a zirconia (ZrO_2) pot with 10 ml ethanol and 12.5g zirconia ball. Wet ball milling was performed on a planetary pulverizer (FRITSCH, Pulverisette 7) at 400 rpm for 10h with reverse rotation every 15min. The obtained slurry was dried at 70 ^oC for 10h. The dried slurry was separated with zirconia ball and pulverized using an agate mortar, and thereafter pelletized at 50 MPa using a hydraulic press machine. The pellet was calcined in a tube furnace at 300 ^oC for 6 h with a fixed Ar flux. The pre-treated pellet was ground using an agate mortar and pelletized again. After calcination at 600 ^oC for 4 h in a

fixed Ar flux, LVFPF was finally obtained.

Characterization of morphology, crystal structure and valence state

The morphology of the as-prepared LVFPF was characterized by using scanning electron microscopy (JEOL, JSM-890) at an acceleration voltage of 15 kV. The composition of the powders was measured with the energy dispersive spectrometer. The crystal structure of the as-prepared LVFPF and charged / discharged phases were measured *ex-situ* on an X-ray diffractometer (RIGAKU, RINT-ULTIMA III) using Cu *K*αradiation (λ= 1.54051Å). The diffraction pattern of pristine electrode and charge / discharged electrodes were recorded in the 2θ range of 10-80 ^{o} and 15-60 ^{o} with a step size of 0.01 ^{o}. Prior to testing, the charged / discharged electrodes were disassembled from the experimental cell and washed several times with ethanol followed by drying at room temperature under vacuum for 5 h. Most of the atomic positions were located according to the results reported by Mba et al.[1, 2] The position of Li atoms was fixed as reported parameters.[1] The crystal structure was further refined by the Rietveld method with the program JANA2006 using the pseudo-Voigt function of Finger *et al* [3, 4] and drawn by the software of VESTA.[5] To determine the occupations of 1a and 1b sites by V and Fe within the lattice structure, the crystallographic information files of $LiV_{0.5}Fe_{0.5}PO_4F$ with different occupations were built by fixing the atomic positions and created by using VESTA. The corresponding X-ray diffraction patterns of these simulated LVFPFs were predicted by using the Reflex program implemented in the software of Materials Studio 6.1 suite.[6] X-ray absorption near edge spectra (XANES) measurements were employed to clarify the valence state and variation of the cations of Fe and V within $Li_xV_{0.5}Fe_{0.5}PO_4F$. Charged / discharged $Li_xV_{0.5}Fe_{0.5}PO_4F$ electrodes were removed from the cell in the glove box, carefully washed with super dehydrated acetonitrile and dried. The dried $Li_{1\pm x}V_{0.5}Fe_{0.5}PO_4F$ electrodes were sealed in laminated packets in an argon-filled glove box. X-ray absorption spectra of $Li_xV_{0.5}Fe_{0.5}PO_4F$ samples and the reference compounds were measured in the energy region of the V and/or Fe *K*-edge at room temperature in transmission mode at the beamline of the SPring-8 synchrotron

radiation facility (BL14B2) in Hyogo, Japan. The intensity of X-ray beam was measured by ionization detectors. Treatment of the raw X-ray absorption data was performed with Athena package.[7] Analysis of V and Fe *K*-edge XANES spectra was performed with the Rigaku REX 2000 program package.[8]

Electrochemical characterization

The electrodes were prepared by mixing the as-prepared LVFPF powder, conductive carbon black (ketjen black) and polytetrafluoroethylene (PTFE) in a weight ratio of 80:15:5. The mixture was ground in an agate mortar for 1 h. Subsequently, the obtained sheet was punched into 10 mm discs. The final electrodes were prepared by pressing the obtained discs onto Al mess, followed by drying at 100 ^{o}C for 8 h under vacuum. Microporous polypropylene membrane was used as separator. 1 mol dm^{-3} solution of $LiClO_4$ in ethylene carbonate / diethyl carbonate (1:1 ratio by volume, all received from Kishida chemical) was applied as electrolyte. The experimental two electrode cells were assembled in an Ar-filled glove box (MIWA). Electrochemical charge / discharge tests were performed at C/50 rate between 2.0 V and 4.7 V at room temperature. Cells for *ex-situ* XRD analysis were charged / discharged to corresponding state at a constant current density of C/50. Cyclic voltammetry was measured using an automatic polarization system (HOKUTO DENKO, HZ-5000) between 2.0 V and 4.7 V at three different scanning rates of 0.05, 0.1 and 0.2 mV s^{-1} at room temperature.

Supplementary results

Table S1. Structural parameters obtained from Rietveld refinement of $LiV_{0.5}Fe_{0.5}PO_4F$.

Atom	Site	*g*	*x*	*y*	*Z*	U_{iso}
*Li	*2i*	1.0	0.7030	0.3710	0.2330	0.015
Fe	*1a*	1.0	0.0000	0.0000	0.0000	0.002
V	*1b*	1.0	0.0000	0.0000	0.5000	0.002
P	*2i*	1.0	0.3157(9)	0.6499(9)	0.2476(9)	0.004
O1	*2i*	1.0	0.3912(18)	0.2533(16)	0.5750(14)	0.007
O2	*2i*	1.0	0.1033(19)	-0.3366(14)	0.3658(15)	0.007
O3	*2i*	1.0	0.6807(17)	0.6540(18)	-0.1487(14)	0.007
O4	*2i*	1.0	0.2690(16)	0.7793(15)	0.0938(15)	0.007
F	*2i*	1.0	-0.1055(15)	0.1028(14)	0.2435(12)	0.007

* The applied atomic position of Li is the same as the parameters reported by Mba et al.[1]

Table S2. Selected atomic distances and polyhedral volumes in $LiV_{0.5}Fe_{0.5}PO_4F$ obtained from Rietveld refinement

Bond type	Average length / Å	Bond type	Average length / Å
V-O1	2.065(9)	Fe -F	1.950(9)
V-O2	1.993(9	P-O1	1.543(9)
Fe-O3	2.018(7)	P-O2	1.58(1)
Fe-O4	2.031(9)	P-O3	1.56(1)
V-F	2.028(9)	P-O4	1.45(1)

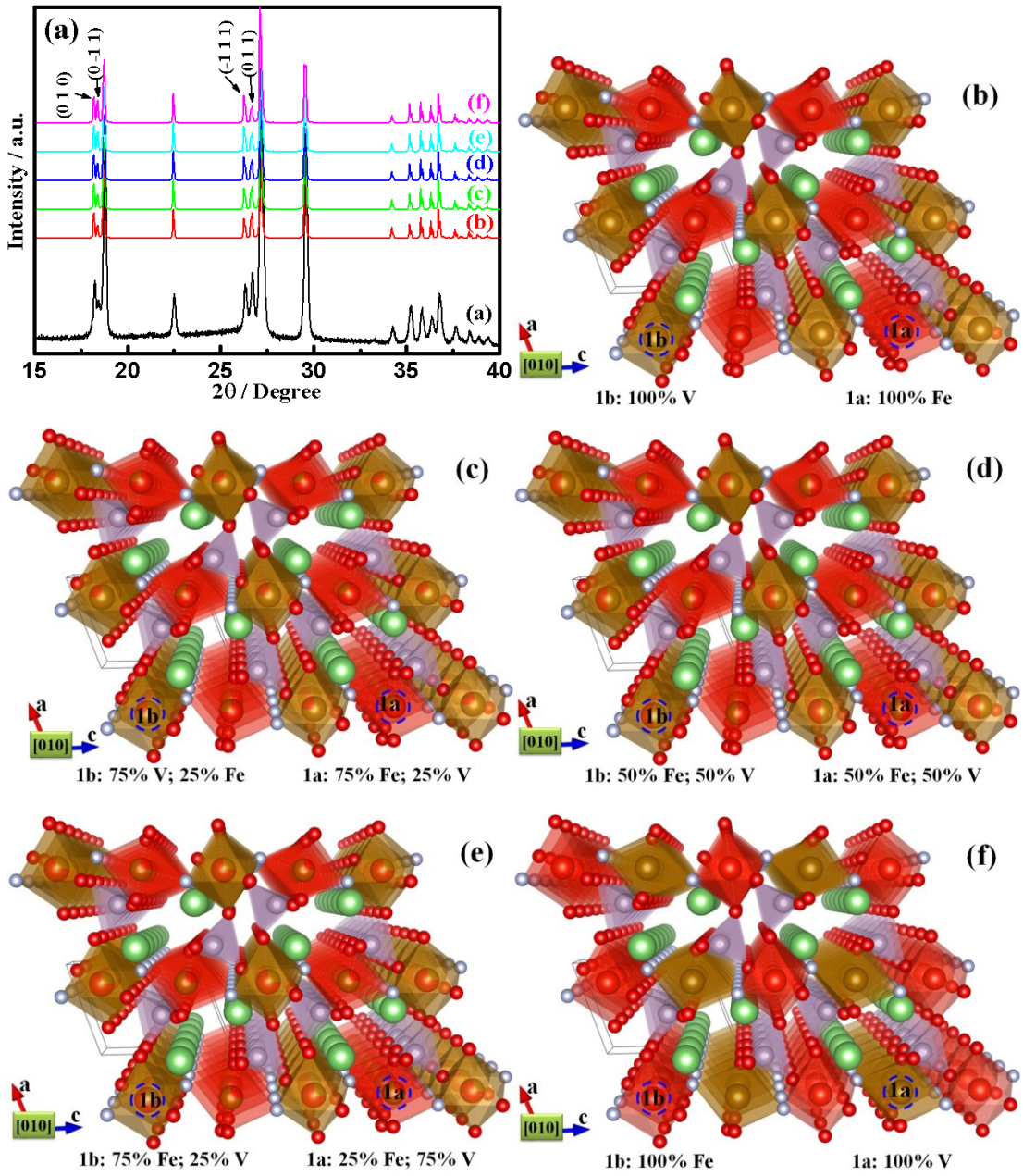

Fig. S1 (a) XRD patterns of the observed $LiV_{0.5}Fe_{0.5}PO_4F$ (Pattern *a*), and the $LiV_{0.5}Fe_{0.5}PO_4F$ calculated based on the cationic site occupation of 1*a* or1*b* site by Fe or V and their corresponding 3D graphic representations: Pattern b and Fig. S1b (1a site：100% Fe; 1b site: 100% V); Pattern c and Fig. S1c (1a site：75% Fe, 25% V; 1b site: 75% V, 25% Fe); Pattern d and Fig. S1d (1a site：50% Fe, 50% V; 1b site: 50% V, 50% Fe); Pattern e and Fig. S1e (1a site：25% Fe, 75% V; 1b site: 25% V, 75% Fe); Pattern f and Fig. S1f (1a site：100% V; 1b site: 100% Fe);

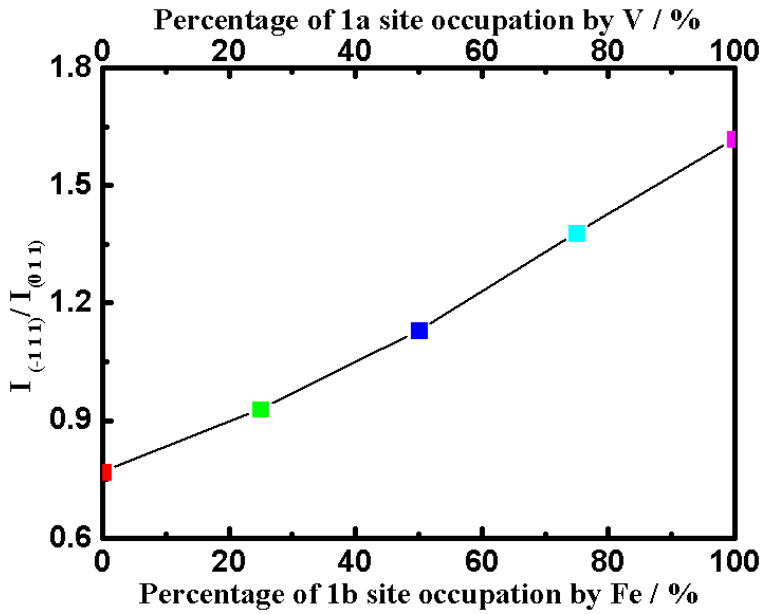

Fig. S2. The linear relation between the peak intensity ratio ($I_{(-1\ 1\ 1)}/I_{(0\ 1\ 1)}$) of the calculated XRD patterns of $LiV_{0.5}Fe_{0.5}PO_4F$ and the site occupation of 1*a* site by V or 1*b* site by Fe, respectively.

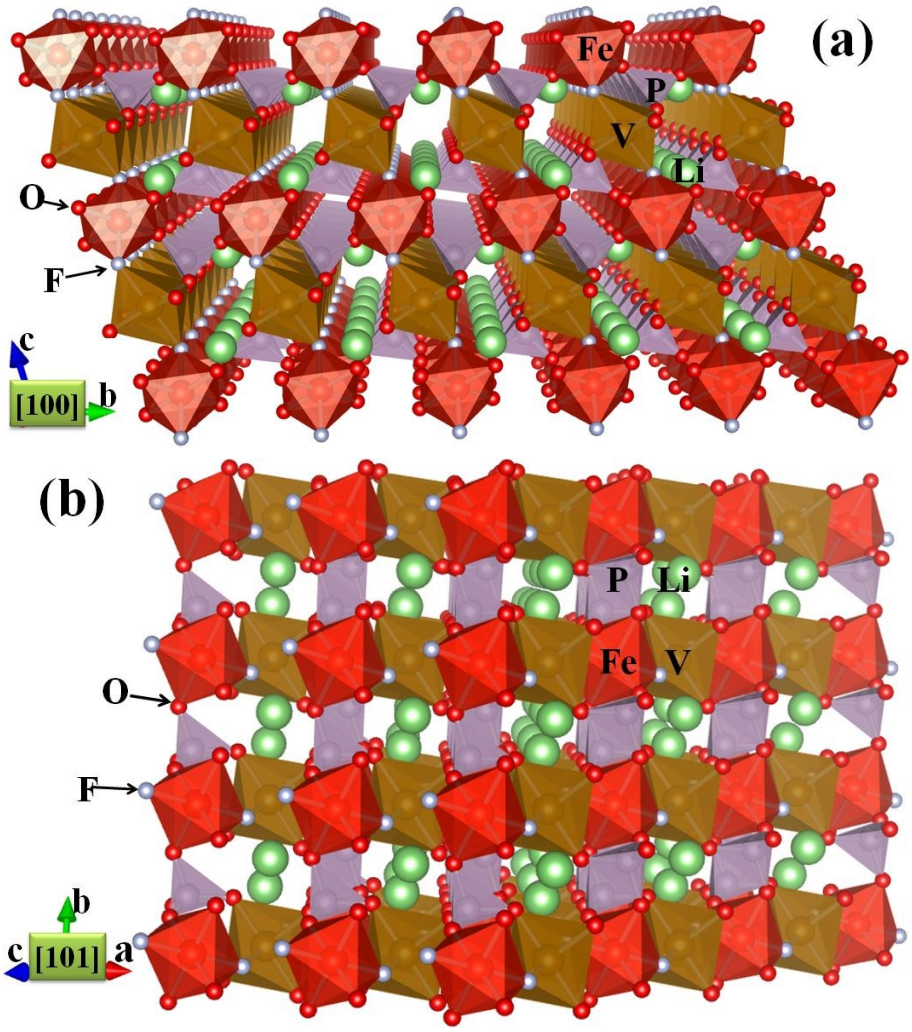

Fig. S3. Graphic representation of a 3D crystal structure of $LiV_{0.5}Fe_{0.5}PO_4F$ projected along (a) [1 0 0] and (b) [1 0 1].

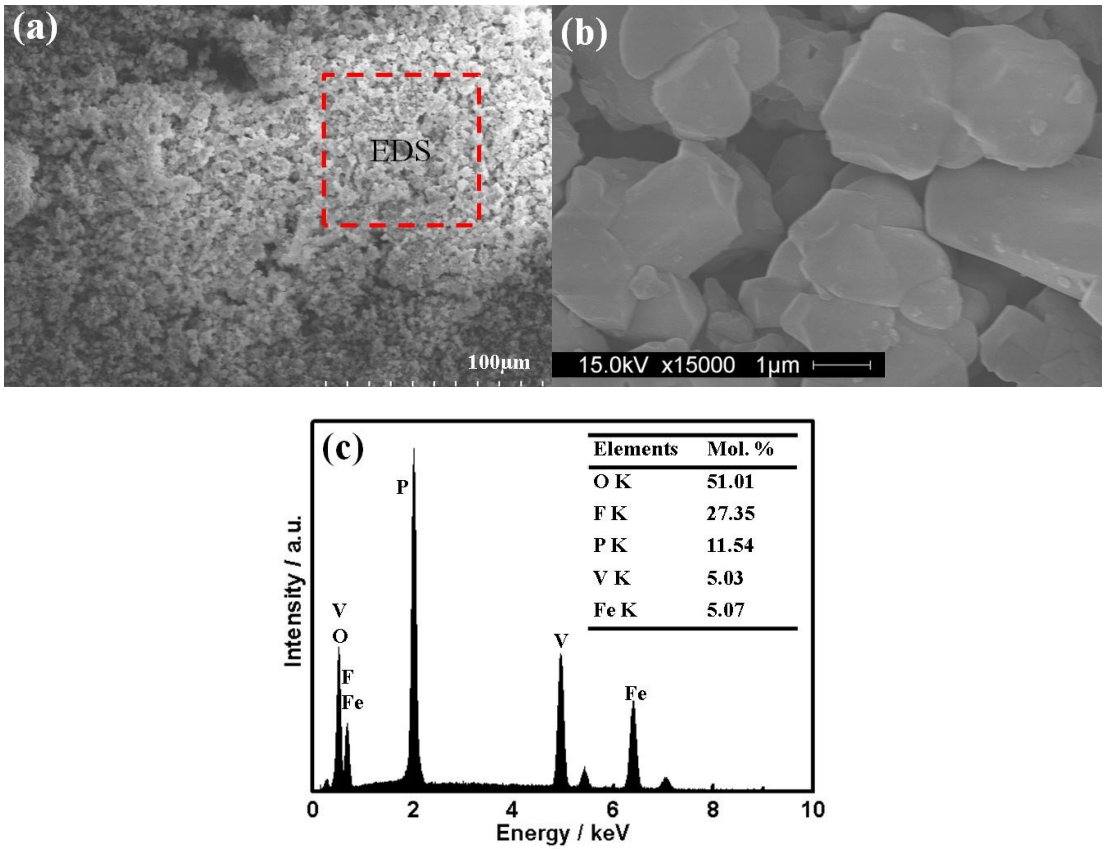

Fig. S4. (a) Low magnification, (b) high magnification SEM images and (c) energy dispersive spectrum analysis results of the as-prepared $LiV_{0.5}Fe_{0.5}PO_4F$

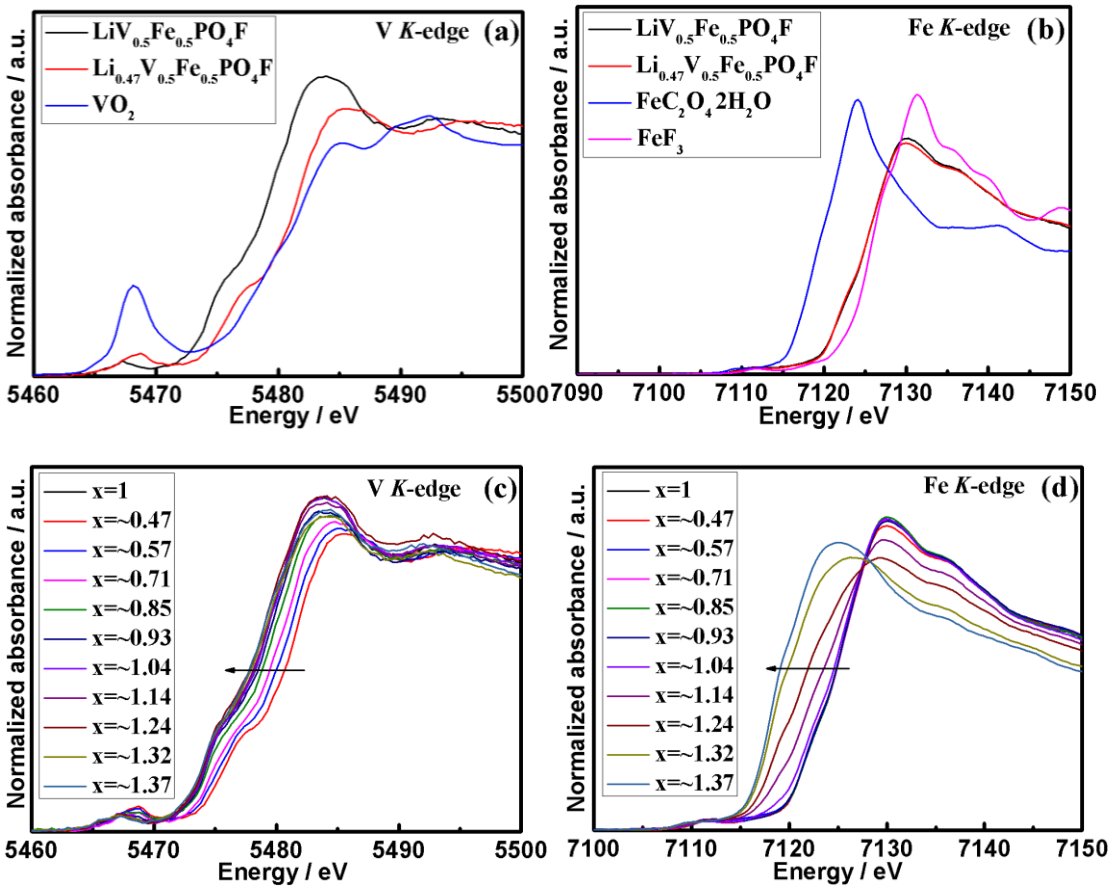

Fig. S5. XANES spectra of $LiV_{0.5}Fe_{0.5}PO_4F$, $Li_{0.47}V_{0.5}Fe_{0.5}PO_4F$ and references compounds at (a) V-*K* edge and (b) Fe-*K* edges; XANES spectra of $Li_xV_{0.5}Fe_{0.5}PO_4F$ at different charge / discharge states at (c) V-*K* edge and (d) Fe-*K* edges.

Table S3. Lattice parameters of $Li_xV_{0.5}Fe_{0.5}PO_4F$ obtained from profile fitting

x	a / Å	b / Å	c / Å	α / °	β / °	γ / °	V / Å^3
1	5.1573(1)	5.2978(2)	7.2409(2)	107.424(3)	107.945(2)	98.431(2)	173.25(1)
0.43	5.1531(13)	5.2409(16)	7.2623(15)	107.360(11)	108.903(12)	97.350(9)	171.53(12)
0.47	5.1585(5)	5.2217(7)	7.2800(8)	107.514(8)	109.254(11)	96.993(9)	171.14(2)
0.67	5.1560(11)	5.2449(11)	7.2601(12)	107.331(9)	108.872(10)	97.546(7)	171.62(9)
0.76	5.1557(9)	5.2893(7)	7.2393(9)	107.399(8)	108.139(8)	98.244(6)	172.83(6)
0.87	5.1563(8)	5.2956(7)	7.2413(8)	107.443(8)	107.990(8)	98.365(6)	173.13(6)
0.96	5.1596(9)	5.2997(8)	7.2431(10)	107.414(8)	108.008(9)	98.253(7)	173.53(7)
1.08	5.1948(20)	5.3266(15)	7.2755(19)	107.475(12)	108.146(0)	97.435(11)	176.87(15)
1.13	5.1896(13)	5.3139(10)	7.2748(15)	107.471(10)	108.276(11)	97.411(10)	176.11(10)
1.32	5.2357(17)	5.3551(12)	7.3052(20)	107.784(9)	108.803(14)	96.383(14)	179.56(13)

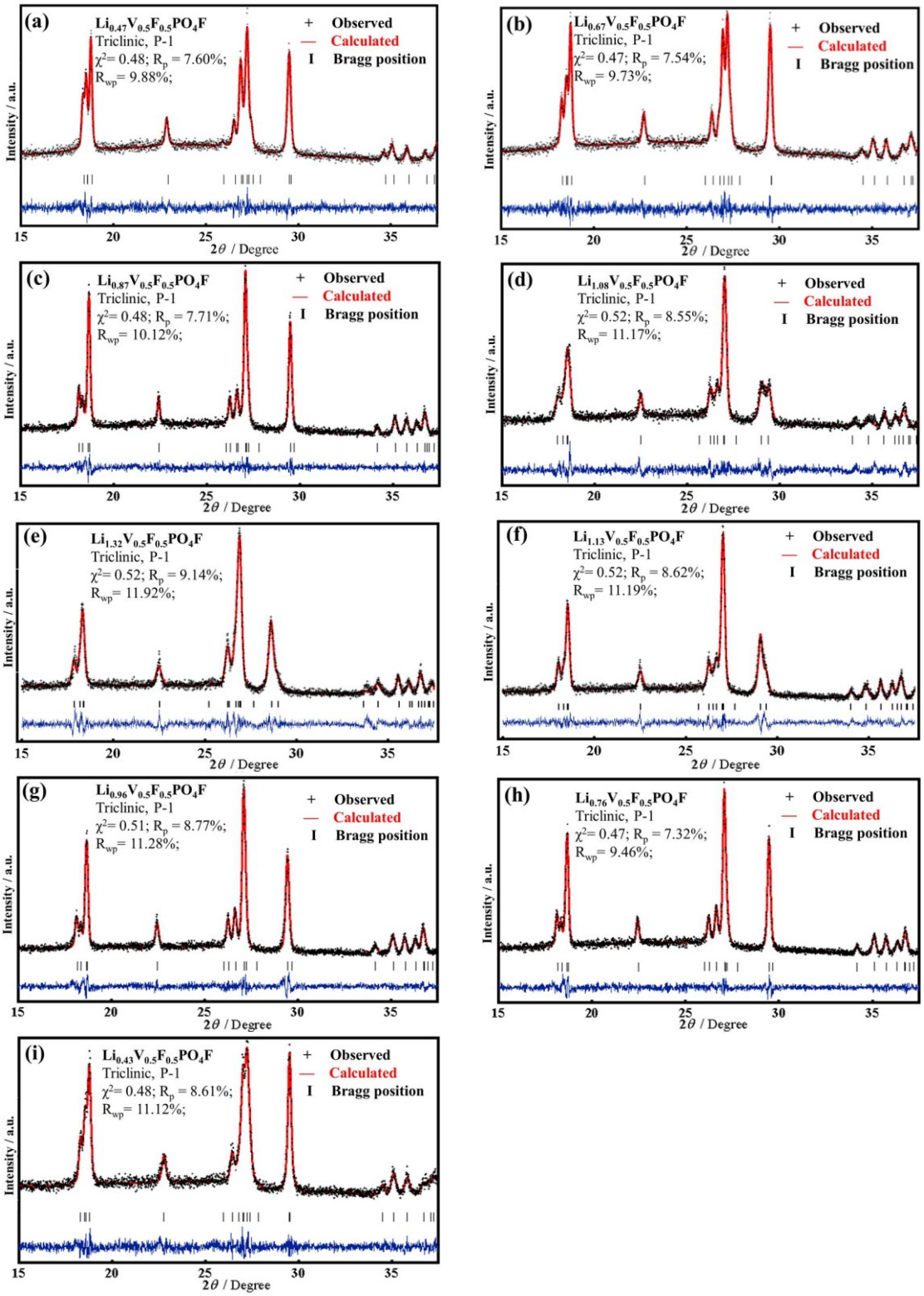

Fig. S6. Profile matching of *ex-situ* X-ray diffraction patterns using Le bail decomposition of $Li_xV_{0.5}Fe_{0.5}PO_4F$ obtained during the 1st discharge process: (a) $x = 0.47$, (b) $x = 0.67$, (c) $x = 0.87$, (d) $x = 1.08$, (e) $x = 1.32$; and obtained during the 2nd charge process: (f) $x = 1.13$, (g) $x = 0.96$, (h) $x = 0.76$, (i) $x = 0.43$.

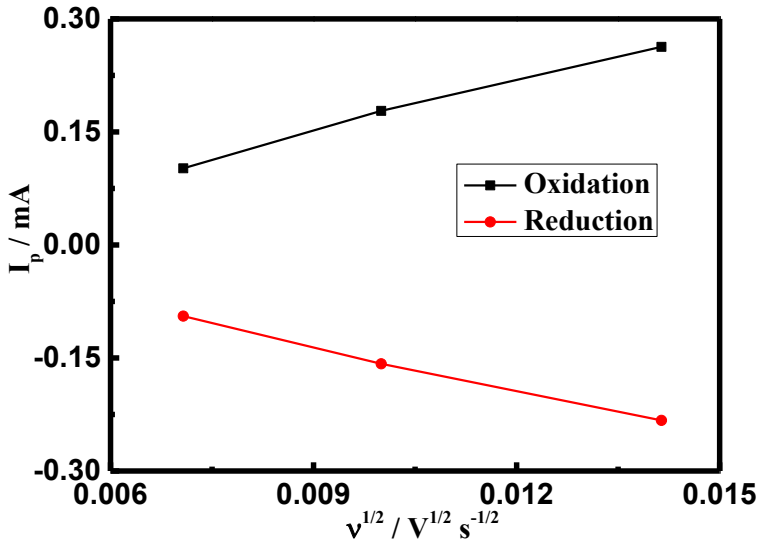

Fig. S7. Plot of peak current (I_p) against the square root of the CV scanning rate showing a linear trend.

References

1 J. M. A. Mba, C. Masquelier, E. Suard, L. Croguennec, Chem. Mater., 2012, **24**, 1223-1234.

2 B. L. Ellis, T. N. Ramesh, L. J. M. Davis, G. R. Goward, L. F. Nazar, Chem. Mater., 2011, **23**, 5138.

3 V. Petrcek, M. Dusek, L. Palatinus, Jana2006-the crystallographic computing system, 2006, Praha, Czech Republic.

4 L.W. Finger, D. E. Cox, A. P. Jephcoat, J. Appl. Cryst., 1994, **27**, 892–900.

5 K. Momma and F. Izumi, J. Appl. Crystallogr., 2008, **41,** 653-658.

6 X. F. Zhou, X. Dong, Z.S. Zhao, A. R. Oganov, Y. J. Tian, and H. T. Wang, Appl. Phys. Lett. 2012, **100,** 061905.

7 B. Ravel and M. Newville, J. Synchrotron Rad., 2005, **12**, 537-541.

8 T Taguchi, T Ozawa and H Yashiro, Phys. Scr. 2005, **T115**, 205-206.